

# The possible existence of Pop III NS-BH binary and its detectability

Tomoya Kinugawa<sup>1</sup>, Takashi Nakamura<sup>2</sup> and Hiroyuki Nakano<sup>2</sup>

<sup>1</sup>*Institute for Cosmic Ray Research, The University of Tokyo, Chiba 277-8582, Japan*

<sup>2</sup>*Department of Physics, Kyoto University, Kyoto 606-8502, Japan*

.....  
In the population synthesis simulations of Pop III stars, many BH (Black Hole)-BH binaries with merger time less than the age of the Universe ( $\tau_H$ ) are formed, while NS (Neutron Star)-BH binaries are not. The reason is that Pop III stars have no metal so that no mass loss is expected. Then, in the final supernova explosion to NS, much mass is lost so that the semi major axis becomes too large for Pop III NS-BH binaries to merge within  $\tau_H$ . However it is almost established that the kick velocity of the order of  $200 - 500 \text{ km s}^{-1}$  exists for NS from the observation of the proper motion of the pulsar. Therefore, the semi major axis of the half of NS-BH binaries can be smaller than that of the previous argument for Pop III NS-BH binaries to decrease the merging time. We perform population synthesis Monte Carlo simulations of Pop III NS-BH binaries including the kick of NS and find that the event rate of Pop III NS-BH merger rate is  $\sim 1 \text{ Gpc}^{-3} \text{ yr}^{-1}$ . This suggests that there is a good chance of the detection of Pop III NS-BH mergers in O2 of Advanced LIGO and Advanced Virgo from this autumn.  
.....

Subject Index      E31, E32, E02, E01, E38

1. *Introduction* The proper-motion observations of pulsars show that the pulsars had the kick velocity in the formation stage. The young pulsars have proper velocity of  $200 - 500 \text{ km s}^{-1}$  [1, 2]. The physical mechanism of such kick velocity may be due to the Harrison-Tademaru mechanism [3], anisotropic emission of neutrinos, anisotropic explosion and so on (see Lorimer [4] for the review). Therefore, it is also reasonable to assume the existence of the proper motion of the pulsars in the formation process of Pop III NSs, although there is no direct evidence since no Pop III star or pulsar is observed. While, Repetto et al. [5] suggest that BHs also have a natal kick velocity comparable to pulsars from the galactic latitude distribution of the low mass X-ray binaries in our galaxy. But, first, this is not the direct observation of proper motion of BHs, and second, since the mass of Pop III BHs is larger than Pop I and Pop II BHs, their kick velocity might be so small that it can be neglected. Therefore, we take into account the natal kick for Pop III NSs but not for Pop III BHs in this paper. The kick speed  $v_k$  obeys a Maxwellian distribution as

$$P(v_k) = \sqrt{\frac{2}{\pi}} \frac{v_k^2}{\sigma_k^2} \exp \left[ -\frac{v_k^2}{\sigma_k^2} \right], \quad (1)$$

where  $\sigma_k$  is the dispersion. The details of the method how to calculate the natal kick are shown in Ref. [6].

In this paper, we perform population synthesis Monte Carlo simulations of Pop III binary stars.

Table 1: The initial distribution functions in this paper.

	Pop III	Pop I,II
IMF	flat ( $10 M_{\odot} < M < 140 M_{\odot}$ )	Salpeter ( $5 M_{\odot} < M < 140 M_{\odot}$ )
IMRF	flat ( $10/M < M_2/M_1 < 1$ )	flat ( $0.1/M < M_2/M_1 < 1$ )
ISF	logflat ( $a_{\min} < a < 10^6 R_{\odot}$ )	logflat ( $a_{\min} < a < 10^6 R_{\odot}$ )
IEF	e ( $0 < e < 1$ )	e ( $0 < e < 1$ )

2. *Brief Explanation of Our Population Synthesis Monte Carlo Simulations* We calculate the Pop III NS-BH and Pop I and II NS-BH for comparison. Pop I and Pop II stars mean solar metal stars and metal poor stars whose metallicity is less than 10% of solar metallicity, respectively. In this paper, we consider five metallicity cases of  $Z = 0$  (Pop III),  $Z = 10^{-2}Z_{\odot}$ ,  $10^{-1.5}Z_{\odot}$ ,  $10^{-1}Z_{\odot}$  and  $Z = 10^{-0.5}Z_{\odot}$ ,  $Z = Z_{\odot}$  (Pop I). There are important differences between Pop III and Pop I and II. Pop III stars are (1) more massive,  $> 10 M_{\odot}$ , (2) smaller stellar radius compared with that of Pop I and II, and (3) no stellar wind mass loss. These properties play key roles in binary interactions.

In order to estimate the event rate of NS-BH mergers and the properties of NS-BH, we use the binary population synthesis method [6–8] which is the Monte Carlo simulation of binary evolution. First, we choose the binary initial conditions such as the primary mass  $M_1$ , the mass ratio  $M_2/M_1$ , the separation  $a$ , and the eccentricity  $e$  when the binary is born. These binary initial conditions are chosen by the Monte Carlo method and the initial distribution functions such as the initial mass function (IMF), the initial mass ratio function (IMRF), the initial separation function (ISF), and the initial eccentricity distribution function (IEF). We adopt these distribution functions for Pop III stars and Pop I and II stars as Table 1. Second, we calculate the evolutions of the primary and secondary stars. If the binary fulfills the condition of binary interaction, we consider binary interactions such as the Roche lobe overflow (RLOF), the common envelope (CE) phase, the tidal effect, the supernova effect, and the gravitational radiation. We treat these binary interactions as our previous studies in Refs. [7, 8]. In this paper, we treat the binary interaction parameter such as the CE parameter  $\alpha\lambda$  and the lose fraction  $\beta$  of transfered stellar matter during a RLOF as  $\alpha\lambda = 1$ ,  $\beta = 0$ , and the conservative core-merger criterion for all models [8]. We adopt the maximum mass of NS is  $3 M_{\odot}$  although this is near the maximum possible ones [9, 10]. We calculate two kick velocity models of  $\sigma_k = 265$  km/s and  $\sigma_k = 500$  km/s.

In order to calculate Pop III binary population synthesis, we use the fitting formulae of Pop III stellar evolution and binary population synthesis code of Refs. [7, 8]. To be more accurate, however, we rewrite the lifetime of the He-burning phase as

$$t_{\text{He}} [\text{yr}] = \begin{cases} 214996 + 543838 \left( \frac{M}{10 M_{\odot}} \right)^{-1} + 64028.1 \left( \frac{M}{10 M_{\odot}} \right)^{-2} + 569484 \left( \frac{M}{10 M_{\odot}} \right)^{-3} \\ \quad (10 M_{\odot} \leq M < 50 M_{\odot}), \\ -108776 + 3213670 \left( \frac{M}{10 M_{\odot}} \right)^{-1} - 5080480 \left( \frac{M}{10 M_{\odot}} \right)^{-2} \\ \quad (20 M_{\odot} \leq M \leq 100 M_{\odot}), \end{cases} \quad (2)$$

---

and define the lifetime of the He-shell burning phase as

$$t_{\text{HeS}} [\text{yr}] = \begin{cases} 54343.2 - 145088 \left( \frac{M}{10 M_{\odot}} \right)^{-1} + 165889 \left( \frac{M}{10 M_{\odot}} \right)^{-2} - 5377.16 \left( \frac{M}{10 M_{\odot}} \right) \\ \quad (10 M_{\odot} \leq M < 50 M_{\odot}), \\ -145220 + 34409.8 \left( \frac{M}{10 M_{\odot}} \right) - 864.4 \left( \frac{M}{10 M_{\odot}} \right)^2 \\ \quad (20 M_{\odot} \leq M \leq 100 M_{\odot}). \end{cases} \quad (3)$$

Thus, we redefine the ignition time of the C burning in Ref. [7] as  $t_{\text{C}}^{\text{b}} = t_{\text{H}} + t_{\text{He}} + t_{\text{HeS}}$ .

On the other hand, in the Pop I and Pop II cases, we use the fitting formulae of Ref. [11] and the formulae of binary interactions in Refs. [7, 8]. We take the magnetic braking in the Pop I and Pop II cases into account, while not for the Pop III case since no magnetic field is usually expected for Pop III star [12–16]. We use the formulae of angular momentum loss by magnetic braking in Ref. [6]. The stellar wind mass loss is effective in Pop I and II stars, while no mass loss in Pop III stars. The stellar wind mass loss makes binary not only light but also wide. In this paper, we treat the stellar wind mass loss for Pop I and II stars as follows. In the case of massive main sequence whose luminosity is more than  $4000 L_{\odot}$ , the strong mass loss is observed. We use the formula of Refs. [11, 17],

$$\dot{M}_{\text{NJ}} = 9.6 \times 10^{-15} \left( \frac{Z}{Z_{\odot}} \right) \left( \frac{R}{R_{\odot}} \right)^{0.81} \left( \frac{L}{L_{\odot}} \right)^{1.24} \left( \frac{M}{M_{\odot}} \right)^{0.16} M_{\odot} \text{ yr}^{-1}. \quad (4)$$

For red giant stars, we use the formulation of Ref. [18],

$$\dot{M}_{\text{R}} = 4 \times 10^{-13} \eta \left( \frac{L}{L_{\odot}} \right) \left( \frac{R}{R_{\odot}} \right) \left( \frac{M}{M_{\odot}} \right)^{-1} M_{\odot} \text{ yr}^{-1}, \quad (5)$$

with  $\eta = 0.5$  where  $\eta$  is the parameter set by the observations of horizontal branch stars in globular clusters [19]. For the asymptotic giant branch stars, we apply the formula of Ref. [20],

$$\log \left( \frac{\dot{M}_{\text{VW}}}{M_{\odot} \text{ yr}^{-1}} \right) = -11.4 + 0.0125 \left[ P_0 - 100 \max \left( \frac{M}{M_{\odot}} - 2.5, 0 \right) \right], \quad (6)$$

where  $P_0$  is Mira pulsation period as

$$\log P_0 = \min \left( 3.3, -2.07 - 0.9 \log \left( \frac{M}{M_{\odot}} \right) + 1.94 \log \left( \frac{R}{R_{\odot}} \right) \right). \quad (7)$$

If the giant star fulfills the Humphreys-Davidson limit ( $L > 10^5 L_{\odot}$  and  $(R/R_{\odot})(L/L_{\odot})^{1/2} > 10^5$ ) [21], the radiation pressure becomes too high and the stellar surface becomes unstable so that the strong mass loss occurs. Giant stars which are near the Humphreys-Davidson limit are called as luminous blue variable (LBV) stars. The stellar wind mass loss rates of LBV stars are typically from  $10^{-5}$  to  $10^{-4} M_{\odot} \text{ yr}^{-1}$ , or  $10^{-3} M_{\odot} \text{ yr}^{-1}$  in the extreme case of  $\eta \text{ Car}$  [22]. In this paper, we adopt the additional mass loss rate,

$$\dot{M}_{\text{LBV}} = 1.5 \times 10^{-4} M_{\odot} \text{ yr}^{-1} \quad (8)$$

for the giants beyond the Humphreys-Davidson limit so that  $\dot{M} = \dot{M} + \dot{M}_{\text{LBV}}$  [6, 23]. After a violent mass loss, the envelope of giant evaporates and the star becomes a naked He star

such as Wolf-Rayet star. We adopt the mass loss rate for Wolf-Rayet like stars as

$$\dot{M}_{\text{WR}} = 10^{-13} L^{1.5} (1.0 - \mu) \left( \frac{Z}{Z_{\odot}} \right)^{0.86} M_{\odot} \text{ yr}^{-1}, \quad (9)$$

where  $\mu$  is

$$\mu = \left( \frac{M - M_{\text{c}}}{M} \right) \min \left\{ 5.0, \max \left[ 1.2, \left( \frac{L}{7.0 \times 10^4 L_{\odot}} \right)^{-0.5} \right] \right\}. \quad (10)$$

This Wolf-Rayet mass loss rate  $\dot{M}_{\text{WR}}$  is a combination of the wind mass loss rate in Ref. [11] and the metal dependent Wolf-Rayet wind in Ref. [24]. For Wolf-Rayet stars, we use the mass loss formula  $\dot{M}_{\text{WR}}(\mu = 0)$ .

**3. Results** In Table 2, we show the number of NS-BH formations and the number of NS-BHs which merge within 15 Gyrs for each metallicity for the initial  $10^6$  binaries. The numbers are for the  $\sigma_{\text{k}} = 265$  km/s models, while the numbers in the parenthesis are for the  $\sigma_{\text{k}} = 500$  km/s models. In the Pop I and Pop II cases, the fraction of NS-BH formation and the fraction of merging NS-BH become larger if the metallicity is lower. In the Pop III case, the initial condition makes binaries easy to be more massive compact objects. Thus, the fraction of NS-BH formation and the fraction of merging NS-BH are larger than those for the Pop I and II cases. In all the metallicity cases, the numbers of NS-BH formation and the numbers of merging NS-BH of the  $\sigma_{\text{k}} = 265$  km/s model are higher than those of the  $\sigma_{\text{k}} = 500$  km/s model due to disruption of the binary for the higher velocity kick. In the case of Pop III in the no kick models, almost all NS-BH cannot merge within the Hubble time in our previous study [7, 8], because they eject a lot of mass at the supernova event, and the separation becomes too wide due to the weak mass loss before the supernova. Thus, in the Pop III case, they need supernova kick in order to merge within the Hubble time.

Figure 1 shows the chirp mass distributions of NS-BH which merge within 15 Gyr for each metallicity. The left and right panels are the  $\sigma_{\text{k}} = 265$  km/s model and the  $\sigma_{\text{k}} = 500$  km/s model for each metallicity, respectively. The chirp mass distributions for the Pop III case are clearly different from those for the Pop I and II cases. The reasons are the difference of BH progenitor evolution and the supernova mass ejection effect. Pop III stars do not lose mass by the stellar wind and the less binary interaction such as the common envelope phase. Thus, the Pop III BHs tends to be more massive than those of Pop I and II. In the case of Pop III NS progenitors, however, since they cannot lose their mass before the supernova due to no wind mass loss and the weak binary interaction, they eject a lot of mass at the supernova event. If the half of total binary mass is ejected at the supernova, the binary disrupts for no kick velocity case. Even though the binary does not disrupt, the orbit becomes wider due to the mass ejection. But, if the companion BH mass is massive, the effect is weak. Thus, the chirp mass of Pop III NS-BH which merges within the Hubble time is more massive than that of Pop I and II. The shapes of chirp mass distributions are changed a little by the kick velocity values. The peak values of chirp mass distributions, however, are not changed although the peak is not so sharp.

We calculated the merger rate of NS-BH. In order to calculate the merger rate, we need the star formation rate for each metallicity. In the Pop III case, we use the star formation rate of Pop III by Ref. [25]. This SFR is calculated by a semi-analytical approach, in which

Table 2: The number of NS-BH formations and the number of NS-BHs which merge within 15 Gyrs for each metallicity for the initial  $10^6$  binaries. The numbers are for the  $\sigma_k = 265$  km/s models, while the numbers in the parenthesis are for the  $\sigma_k = 500$  km/s models.

$Z$	$Z_\odot$	$10^{-0.5}Z_\odot$	$10^{-1}Z_\odot$	$10^{-1.5}Z_\odot$	$10^{-2}Z_\odot$	0
NS-BH	148 (32)	598 (169)	1296 (416)	1686 (576)	1896 (617)	22638 (11192)
merging NS-BH	15 (2)	191 (67)	525 (213)	755 (377)	862 (401)	9089 (5856)

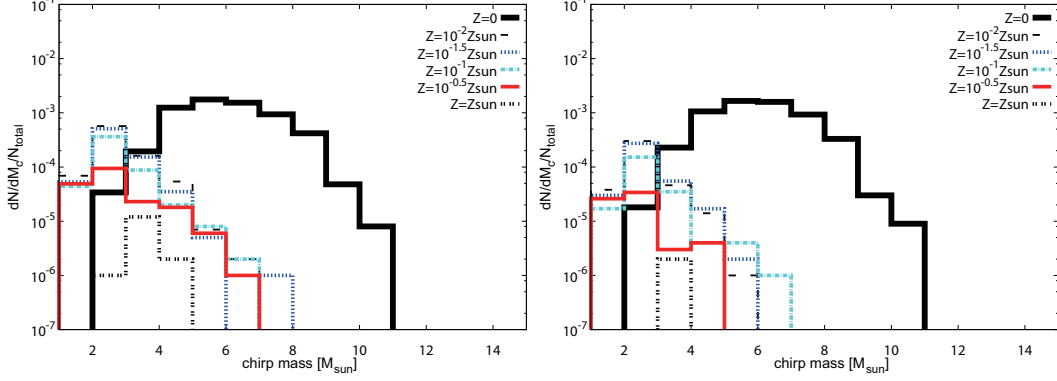


Fig. 1: The chirp mass distributions of NS-BH for each metallicity. The left and the right panels are the  $\sigma_k = 265$  km/s and  $\sigma_k = 500$  km/s models for each metallicity, respectively.

the following effects are considered: (1) the radiative feedback on Pop III star formation, (2) the inhomogeneous re-ionization of the intergalactic medium (IGM), and (3) the chemical pollution of the IGM. <sup>1</sup> Using Pop III binary population synthesis results and the Pop III SFR, the merger rate density of Pop III NS-BH  $R_{\text{NS-BH}}(t)$  [ $\text{yr}^{-1} \text{Gpc}^{-3}$ ] is calculated as

$$R_{\text{PopIII}}(t) = \int_0^t \frac{f_b}{1 + f_b} \frac{SFR(t')}{\langle M \rangle} \frac{N_{\text{NS-BH}}(t - t')}{N_{\text{total}}} dt', \quad (11)$$

where  $f_b$ ,  $SFR(t')$ ,  $N_{\text{NS-BH}}(t - t')$ ,  $\langle M \rangle$  and  $N_{\text{total}}$  are the binary fraction, the star formation rate of Pop III at  $t'$ , the number of NS-BHs which merge from  $t'$  to  $t$ , the average mass, and the total number of the binary. We use  $f_b = 0.5$ ,  $\langle M \rangle = 75 M_\odot$ ,  $N_{\text{total}} = 10^6$ . On the other hand, for the SFR of Pop I and II, we use the SFR calculated by the observation [29],

$$\Psi(z) = 1.5 \times 10^{-2} \frac{(1 + z)^{2.7}}{1 + \left[\frac{1+z}{2.9}\right]^{5.6}} M_\odot \text{yr}^{-1} \text{Mpc}^{-3}, \quad (12)$$

in  $0 < z \lesssim 8$ . To decide the metallicity change as a function of the redshift, we use the formula of galaxy mass-metallicity relation calculated by simulation [30],

$$\log \left( \frac{Z_*}{Z_\odot} \right) = 0.40 \left[ \log \left( \frac{M_*}{M_\odot} \right) - 10 \right] + 0.67 \exp(-5.0z) - 1.04, \quad (13)$$

<sup>1</sup> Recently, some researchers calculated the Pop III SFR using the optical depth of Thomson scattering observed by Planck [26–28]. Their SFRs are several or ten times lower than our SFR, while they depend on the adopted optical depth, the escape fraction of ionizing photons, IMF and the mass range.

Table 3: NS-BH merger rates at the present day [ $\text{yr}^{-1} \text{Gpc}^{-3}$ ].

$Z$	$Z_{\odot}$	$10^{-0.5}Z_{\odot}$	$10^{-1}Z_{\odot}$	$10^{-1.5}Z_{\odot}$	$10^{-2}Z_{\odot}$	Pop I,II sum	0
$\sigma_k = 265 \text{ km/s}$	0.457	16.1	2.57	0.523	0.0623	19.7	1.25
$\sigma_k = 500 \text{ km/s}$	0.158	5.16	1.06	0	0	6.38	0.956

in  $0 < z < 6$ , and the galaxy mass distribution fitted by the Schechter function [31] as

$$\phi_{\text{sh}}(M)dM = \phi^* \left( \frac{M}{M^*} \right)^{\alpha} \exp \left( -\frac{M}{M^*} \right) \frac{dM}{M^*}, \quad (14)$$

where

$$\phi^*(z) = 3.5 \times 10^{-3} (1+z)^{-2.2}, \quad (15)$$

$$\log M^*(z) = 11.16 + 0.17z - 0.07z^2, \quad (16)$$

$$\alpha(z) = -1.18 - 0.082z, \quad (17)$$

in  $0 < z < 4$ . To calculate the metallicity evolution  $z < 8$ , we extrapolate Eqs. (13) and (14). We decided the metallicity switching redshift as the intermediate value in log as  $Z = 10^{-1.75}$  ( $z = 6.745$ ),  $Z = 10^{-1.25}$  ( $z = 5.168$ ),  $Z = 10^{-0.75}$  ( $z = 2.528$ ), and  $Z = 10^{-0.25}$  ( $z = 0.096$ ). Using binary population synthesis results, the SFRs and the metallicity, the merger rates of each metallicity  $R_{Z, \text{NS-BH}}$  are given by

$$R_{Z, \text{NS-BH}}(t) = \int_0^t \frac{f_b}{1+f_b} \frac{\text{SFR}(Z, t')}{\langle M \rangle} \frac{\int_{5M_{\odot}}^{140M_{\odot}} \text{IMF}(M)dM}{\int_{0.1M_{\odot}}^{140M_{\odot}} \text{IMF}(M)dM} \frac{N_{Z, \text{NS-BH}}(t-t')}{N_{\text{total}}} dt'. \quad (18)$$

where  $f_b = 0.5$  and  $\langle M \rangle = 0.355 M_{\odot}$ .

Figures 2 and 3 present the merger rate densities of NS-BH. Table 3 shows the NS-BH merger rates at the present day for each metallicity and Pop I and II summation. In the Pop I and II cases,  $Z = 10^{-0.5}Z_{\odot}$  contributes the most of the merger rate.

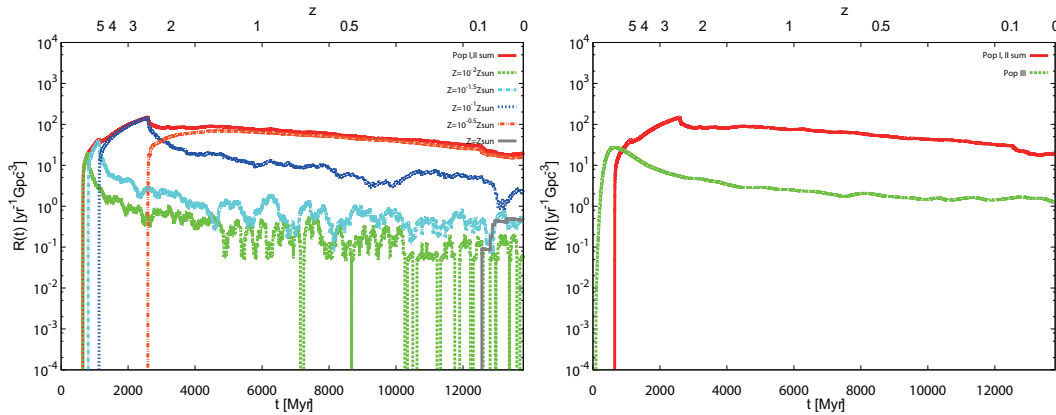


Fig. 2: The merger rate density of NS-BH for the  $\sigma_k = 265 \text{ km/s}$  model. The left panel shows the merger rate densities of Pop I and II, and Pop I and II summation. The right panel shows the merger rate densities of summation of Pop I and II, and Pop III.

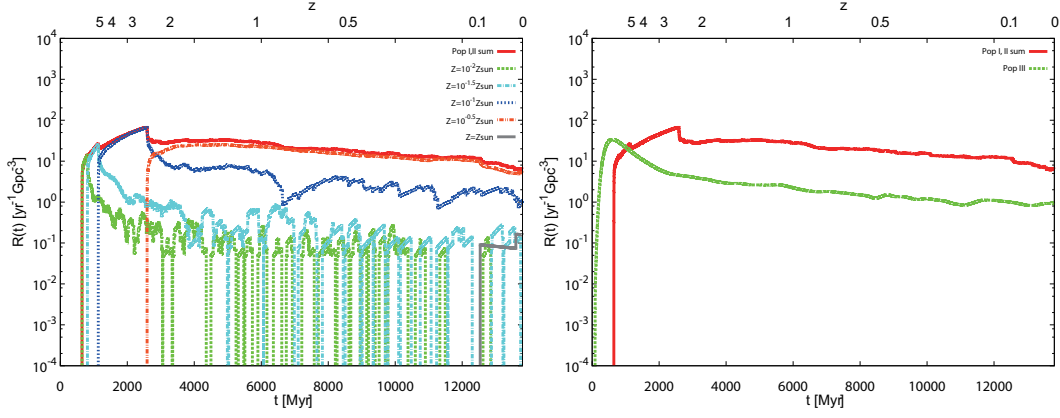


Fig. 3: This figure is same as Fig. 2 but for the  $\sigma_k = 500$  km/s model.

4. *Discussions* The NS-BH merger might be detected not only by a gravitational wave, but also electromagnetic waves. When a NS merges a BH, the NS is possibly disrupted by the tidal force from the BH. At that time, the electromagnetic radiation is emitted due to the r-process. This phenomenon is called as the kilonova. In the case of massive BHs such as  $\sim 30 M_\odot$ , the kilonova does not occur generally since the NS is sucked into the BH before the tidal disruption fully occurs. However, if the spin of BH is high, it is conceivable that the tidal disruption can occur. Figure 4 shows the BH mass and spin distributions of merging Pop III NS-BH. The BH mass is massive, but a half of BHs have the extreme high spin. Thus, they can produce the kilonova. Of course, since the NS kick makes the orbit misalign with the spin of BH, only the component of BH spin projected to the orbit is effective [32]. But, in the case of merging NS-BH, the kick velocity is low and such misalignment effect is not so effective. In order to consider the most misalign case, we assume that there is no mass loss at the supernova, and that the direction of the natal kick is the direction orthogonal to the orbit. In order to avoid the disruption, the kick speed of the NS-BH progenitor  $v_k$  should satisfy  $v_{\text{esc}}^2 > v_o^2 + v_k^2$  where  $v_{\text{esc}}$  and  $v_o$  are the escape speed and the orbit speed before the supernova, respectively. For simplicity, we assume no mass loss at the supernova. The escape speed becomes  $v_{\text{esc}}^2 = 2v_o^2$ . Thus,  $v_k < v_o$  and the misalignment angle  $\theta < 45^\circ$ . If the spin of BH is  $\sim 1$ , the effective spin is larger than  $\cos 45^\circ = 0.7$ . Furthermore, actually the mass loss occurs at the supernova, and  $v_{\text{esc}}$  is lower than that of no mass loss case. Thus, the misalignment angle is much lower than that of no mass loss case and the effective spin of BH is much larger than that of no mass loss case. Therefore, the misalignment of kick is not effective.

Finally, in Table 4, we show the NS-BH event rates [ $\text{yr}^{-1}$ ] by using the expected noise of Advanced LIGO. Here, we used the fitting noise curve presented in Ref. [33] for the design sensitivity which gives the average distance  $\sim 200$  Mpc for binary NS coalescences with two  $1.4M_\odot$  NSs, and for O2 where we assume the average distance  $\sim 100$  Mpc and half the design sensitivity [34]. As for the NS-BH merger rates, we adopted the values at the present day given in Table 3 for  $\sigma_k = 265$  km/s. The detailed calculation of the inspiral-merger-ringdown waveforms is summarized in Ref. [35], based on Refs. [36, 37]. As the assumption of the chirp mass  $M_c$  of the inspiral phase, we fixed  $M_c = 2M_\odot$  (assuming  $M_1 = 3.97M_\odot$  and  $M_2 = 1.4M_\odot$ ) and  $6M_\odot$  (assuming  $M_1 = 53.9M_\odot$  and  $M_2 = 1.4M_\odot$ ) for Pop I and II,



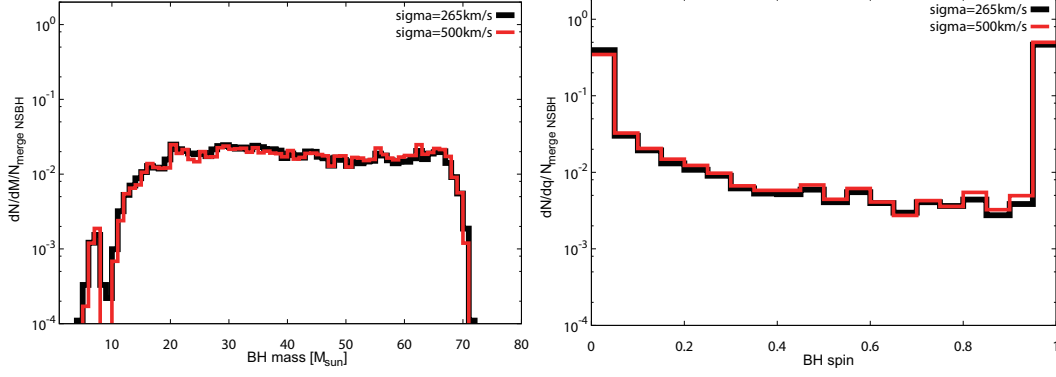


Fig. 4: The left panel shows the BH mass of Pop III NS-BH which merge within 15 Gyr. The right panel shows the BH spin of Pop III NS-BH which merge within 15 Gyr.

Table 4: NS-BH event rates for O2 by Advanced LIGO. The numbers in the parenthesis denote those for the design sensitivity. The maximum redshift  $z_{\max}$  (and the luminosity distance  $d_{L,\max}$ ) is obtained by setting the averaged SNR = 8.

$Z$	$z_{\max}$	$d_{L,\max}$ [Mpc]	Event rate [ $\text{yr}^{-1}$ ]
Pop I, II sum	0.0352 (0.0706)	155 (318)	0.269 (2.06)
0, BH spin $\sim 0$	0.108 (0.216)	500 (1070)	0.445 (3.06)
0, BH spin $\sim 1$	0.124 (0.264)	580 (1340)	0.658 (5.24)

and Pop III, respectively. Although there is no contribution to the signal-to-noise ratio (SNR) from the merger and ringdown phases for Pop I and II, we find for Pop III that the ringdown phase contributes the SNR and the difference in the remnant BH spin is also important. Therefore, we give two cases, the BH spin  $\sim 0$  and 1 (see the right panel of Fig. 4), in Table 4. The detection rate of Pop III NSBH is larger than that of Pop I and II, although the Pop III NSBH rate depends on the uncertainty of the Pop III SFR. The chirp mass of Pop III NSBH is clearly more massive than that of Pop I and II. Thus, we might distinguish the Pop III NSBH from NSBH of Pop I and II.

*Acknowledgment* This work was supported by MEXT Grant-in-Aid for Scientific Research on Innovative Areas, “New Developments in Astrophysics Through Multi-Messenger Observations of Gravitational Wave Sources”, No. 24103006 (TN, HN), by the Grant-in-Aid from the Ministry of Education, Culture, Sports, Science and Technology (MEXT) of Japan No. 15H02087 (TN), and JSPS Grant-in-Aid for Scientific Research (C), No. 16K05347 (HN).

## References

- [1] A. G. Lyne and D. R. Lorimer, *Nature* **369**, 127 (1994).
- [2] B. M. S. Hansen and E. S. Phinney, *Mon. Not. Roy. Astron. Soc.* **291**, 569 (1997) [astro-ph/9708071].
- [3] E. R. Harrison and E. P. Tademaru, *Astrophys. J.* **201**, 447 (1975).
- [4] D. R. Lorimer, *Living Rev. Rel.* **11**, 8 (2008) [arXiv:0811.0762 [astro-ph]].
- [5] S. Repetto, M. B. Davies and S. Sigurdsson, *Mon. Not. Roy. Astron. Soc.* **425**, 2799 (2012) [arXiv:1203.3077 [astro-ph.GA]].



- 
- [6] J. R. Hurley, C. A. Tout and O. R. Pols, Mon. Not. Roy. Astron. Soc. **329**, 897 (2002) [astro-ph/0201220].
  - [7] T. Kinugawa, K. Inayoshi, K. Hotokezaka, D. Nakauchi and T. Nakamura, Mon. Not. Roy. Astron. Soc. **442**, 2963 (2014) [arXiv:1402.6672 [astro-ph.HE]].
  - [8] T. Kinugawa, A. Miyamoto, N. Kanda and T. Nakamura, Mon. Not. Roy. Astron. Soc. **456**, 1093 (2016) [arXiv:1505.06962 [astro-ph.SR]].
  - [9] C. E. Rhoades, Jr. and R. Ruffini, Phys. Rev. Lett. **32**, 324 (1974).
  - [10] J. B. Hartle, Phys. Rep, **46**, 201 (1978)
  - [11] J. R. Hurley, O. R. Pols and C. A. Tout, Mon. Not. Roy. Astron. Soc. **315**, 543 (2000) [astro-ph/0001295].
  - [12] R. E. Pudritz, & J. Silk, Astrophys. J. **342**, 650 (1989)
  - [13] R. M. Kulsrud, R. Cen, J. P. Ostriker and D. Ryu, Astrophys. J. **480**, 481 (1997) [astro-ph/9607141].
  - [14] L. M. Widrow, Rev. Mod. Phys. **74**, 775 (2002) [astro-ph/0207240].
  - [15] M. Langer, J. L. Puget and N. Aghanim, Phys. Rev. D **67**, 043505 (2003) [astro-ph/0212108].
  - [16] K. Doi and H. Susa, Astrophys. J. **741**, 93 (2011) [arXiv:1108.4504 [astro-ph.CO]].
  - [17] H. Nieuwenhuijzen and C. de Jager, Astron. Astrophys. **231**, 134 (1990).
  - [18] R. P. Kudritzki and D. Reimers, Astron. Astrophys. **70**, 227 (1978).
  - [19] I. Iben, Jr. and A. Renzini, Ann. Rev. Astron. Astrophys. **21**, 271 (1983).
  - [20] E. Vassiliadis and P. R. Wood, Astrophys. J. **413**, 641 (1993).
  - [21] R. M. Humphreys and K. Davidson, Publ. Astron. Soc. Pac. **106**, 1025 (1989).
  - [22] N. Smith, Ann. Rev. Astron. Astrophys. **52**, 487 (2014) [arXiv:1402.1237 [astro-ph.SR]].
  - [23] K. Belczynski, T. Bulik, C. L. Fryer, A. Ruiter, J. S. Vink and J. R. Hurley, Astrophys. J. **714**, 1217 (2010) [arXiv:0904.2784 [astro-ph.SR]].
  - [24] J. S. Vink and A. de Koter, Astron. Astrophys. **442**, 587 (2005) [astro-ph/0507352].
  - [25] R. S. de Souza, N. Yoshida and K. Ioka, Astron. Astrophys. **533**, A32 (2011) [arXiv:1105.2395 [astro-ph.CO]].
  - [26] E. Visbal, Z. Haiman and G. L. Bryan, Mon. Not. Roy. Astron. Soc. **453**, 4456 (2015) [arXiv:1505.06359 [astro-ph.CO]].
  - [27] T. Hartwig, M. Volonteri, V. Bromm, R. S. Klessen, E. Barausse, M. Magg and A. Stacy, Mon. Not. Roy. Astron. Soc. **460**, L74 (2016) [arXiv:1603.05655 [astro-ph.GA]].
  - [28] K. Inayoshi, K. Kashiyama, E. Visbal and Z. Haiman, Mon. Not. Roy. Astron. Soc. **461**, 2722 (2016) [arXiv:1603.06921 [astro-ph.GA]].
  - [29] P. Madau and M. Dickinson, Ann. Rev. Astron. Astrophys. **52**, 415 (2014) [arXiv:1403.0007 [astro-ph.CO]].
  - [30] X. Ma, P. F. Hopkins, C. A. Faucher-Giguere, N. Zolman, A. L. Muratov, D. Keres and E. Quataert, Mon. Not. Roy. Astron. Soc. **456**, 2140 (2016) [arXiv:1504.02097 [astro-ph.GA]].
  - [31] A. Fontana *et al.*, Astron. Astrophys. **459**, 745 (2006) [astro-ph/0609068].
  - [32] K. Kawaguchi, K. Kyutoku, H. Nakano, H. Okawa, M. Shibata and K. Taniguchi, Phys. Rev. D **92**, 024014 (2015) [arXiv:1506.05473 [astro-ph.HE]].
  - [33] D. Keppel and P. Ajith, Phys. Rev. D **82**, 122001 (2010) [arXiv:1004.0284 [gr-qc]].
  - [34] J. Aasi *et al.* [LIGO Scientific and VIRGO Collaborations], Living Rev. Rel. **19**, 1 (2016) [arXiv:1304.0670 [gr-qc]].
  - [35] T. Nakamura *et al.*, arXiv:1607.00897 [astro-ph.HE].
  - [36] N. Dalal, D. E. Holz, S. A. Hughes and B. Jain, Phys. Rev. D **74**, 063006 (2006) [astro-ph/0601275].
  - [37] P. Ajith *et al.*, Phys. Rev. Lett. **106**, 241101 (2011) [arXiv:0909.2867 [gr-qc]].

This figure "mergingNSBHchirpmass.jpg" is available in "jpg" format from:

<http://arxiv.org/ps/1610.00305v1>